Differential Error Feedback Active Noise Control with the Auxiliary Filter based Mapping Method

Chuang Shi, Feiyu Du, Chunyu Liu, and Huiyong Li

***Abstract*—This letter proposes a differential error feedback active noise control (FBANC) system in an open end duct to mitigate interferences from its downstream. The interference waves entering the duct cause disturbance to the conventional FBANC controller and even result in divergence of the control filter. This is due to the omni-directivity of the error microphone. The differential microphone array (DMA) can be constructed in a compact size using only one more omni-directional microphone. The DMA forms a frequency-invariant beampattern that presents configurable nulls. When the output of the DMA is used as the error signal, the null can be designed to enhance the robustness of the FBANC system against interferences. However, this differential error signal is converted from the sound pressure gradient instead of the sound pressure. The DMA's location does not precisely indicate the control point where optimum noise reduction has been achieved. To solve this problem, an auxiliary filter based mapping (AFMap) method is developed to map the differential error signal to the location of an omni-directional microphone in the DMA. Experiment results demonstrate that the proposed differential error FBANC system is much less sensitive to interferences than the conventional FBANC system, and the AFMap method can ensure optimum noise reduction occurring at the target control point.**

***Index Terms*—Active noise control, differential microphone array, auxiliary filter, internal model control**

I. Introduction

THE goal of active noise control (ANC) is to reduce undesirable noise by creating an anti-noise wave [1]–[3]. In order for the anti-noise wave to have the same amplitude and opposite phase as the noise wave, ANC systems have been developed with the feedforward, feedback, and hybrid structures [4]–[6].

A feedforward ANC system consists of reference microphones, secondary sources and error microphones. The reference microphones provide the reference signal that enables the feedforward ANC system to control the broadband noise [7]–[10]. In contrast, the feedback ANC (FBANC) system consists of secondary sources and error microphones only. Its reference signal is conventionally synthesized by the internal model control (IMC) method [11], [12]. The FBANC system is often deployed to control the narrowband noise, which exhibits high auto-correlations with long lags [13], [14]. The hybrid ANC system combines the feedforward and feedback ANC structures, aiming at reducing the broadband and narrowband noises at the same time [15], [16].

This manuscript is jointly supported by the National Natural Science Foundation of China and the Civil Aviation Administration of China (Joint Grant No. U1933127).

The authors are with the School of Information and Communication Engineering, University of Electronic Science and Technology of China, Chengdu, China.

Corresponding author's email: shichuang@uestc.edu.cn

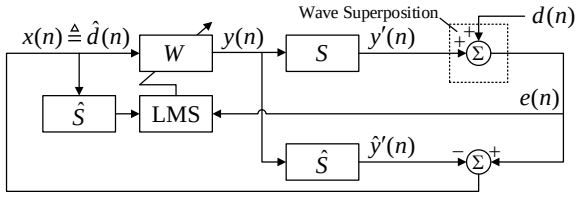

Fig. 1. Block diagram of a conventional IMC-based single-channel FBANC system.

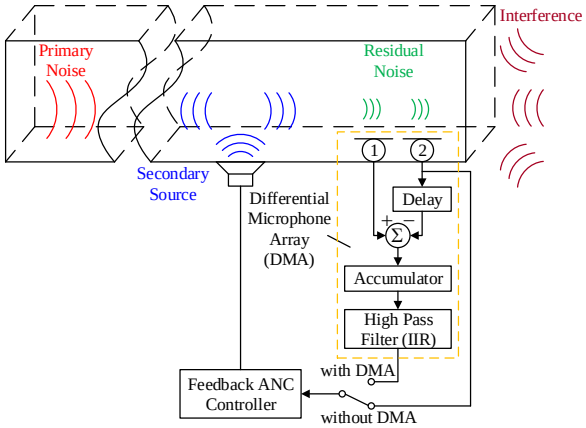

Fig. 2. FBANC system in a duct with a switch to illustrate the comparison between the conventional error signal and the differential error signal.

The FBANC system is preferable for its compact size. Figure 1 shows a single-channel FBANC system. The coefficients of the control filter are adaptively updated to minimize the square of the error signal by the filtered-x least mean squares (FxLMS) algorithm [17]–[19]. Therefore, the error microphone is necessarily placed at the target control point, where optimum noise reduction should be achieved [20], [21].

Figure 2 illustrates the FBANC system implemented in an open end duct. The single-channel FBANC system is adequate to mitigate the noise coming from the upstream, if the noise frequency is below the cut-off frequency of the duct [22]. When the interference waves, which may contain frequency components higher than the cut-off frequency of the duct, enter the duct from the open end, the auto-correlativity of the error signal deteriorates. This can interrupt the conventional FBANC controller, even resulting in the divergence of the control filter. Hence, a directional error microphone that pinpoints the upstream and suppresses interferences is highly desirable.

Among various techniques to extract directional sound of

interest, the differential microphone array (DMA) is advantageous in its frequency-invariant beampattern, and can be constructed within a compact size using a minimum of 2 omni-directional microphones [23]–[29]. The DMA responds to the acoustic spatial pressure difference between two closely-spaced points in space, which measures the sound pressure gradient instead of the sound pressure [30]–[32]. When the output of the DMA is used as the error signal in the FBANC system, the DMA's location does not precisely indicate the control point where optimum noise reduction has been achieved.

To solve this problem, an auxiliary filter based mapping method (AFMap) is developed. The auxiliary filter method was originally proposed in the virtual sensing technique, whereby noise reduction is equivalently achieved when the error microphone cannot be permanently placed at the target control point, but a monitoring microphone works non-stop at a different location [33]–[40]. In contrast with the virtual sensing technique, the differential error signal does not present sound pressures of any microphones in the FBANC system. The AFMap method proposed in this letter is dedicated to allocating the control point at the location of an omni-directional microphone in the DMA. Both the differential error signal and the output of the omni-directional microphone are available to the FBANC system. However, only the former is configurable to be free from interferences.

The main contributions of this letter are summarized below: 1) a feedback structure using the output of a DMA as the error signal is proposed to enhance the robustness of the FBANC system against interferences; 2) the AFMap method is developed to map the differential error signal to the precise location of an omni-directional microphone in the DMA, in order for the control point to be easily localized; 3) experiments are carried out in an open end duct to demonstrate the effectiveness of the proposed structure and the AFMap method.

II. Feedback Active Noise Control System Using The Differential Microphone Array

A. Conventional IMC-based FBANC system

In Fig.1, the input of the control filter $x(n)$ is the estimate of the disturbance signal $\hat{d}(n)$, *i.e.*

$$x(n) \triangleq \hat{d}(n) = e(n) - \hat{\mathbf{s}}(n) * \mathbf{y}(n), \tag{1}$$

where $e(n)$ is the error signal; $\hat{\mathbf{s}}(n)$ is the secondary path model; $*$ denotes the convolution operation; $\mathbf{y}(n) = [y(n), y(n-1), \ldots, y(n-N+1)]^T$ is the control signal vector, of which the dimension is denoted as N and the superscript T denotes the transpose operator.

The output of the control filter is written as

$$y(n) = \mathbf{w}^T(n)\mathbf{x}(n), \tag{2}$$

where $\mathbf{w}(n)$ is the control filter and the reference signal vector is formed as $\mathbf{x}(n) = [x(n), x(n-1), \ldots, x(n-N+1)]^T$.

The control filter coefficients are adaptively updated by the FxLMS algorithm as

$$\mathbf{w}(n+1) = \mathbf{w}(n) - \mu_w[\hat{\mathbf{s}}(n) * \mathbf{x}(n)]e(n), \tag{3}$$

where μ_w is the step size.

B. Differential error FBANC system

To construct the DMA, an additional omni-directional microphone (microphone 1) is placed closely in front of the conventional error microphone (microphone 2) as shown in Fig. 2. Both of them can conduct noise monitoring at the same time. They receive the primary noise and the interference with distinct time difference. Hence, the interference can be suppressed by subtracting a properly delayed output of microphone 2 from the output of microphone 1. The delay is designed to compensate for the relative time delay between the two microphones resultant from the propagation of the interference. It is usually not a multiple of the sampling interval because the spacing between the two microphones is much smaller than the wavelength of the primary noise. Hence, a fractional delay filter is adopted to implement this delay [41].

After the differential operation, although the interference is suppressed, the primary noise is high-pass filtered. An integrator is needed to recover the spectrum of the primary noise. The integrator is realized by an accumulator in the digital domain when the noise frequency is relatively low. The frequency response of the accumulator is written as

$$H_{acc}(e^{j\omega}) = \frac{1}{1 - e^{-j\omega}} \approx \frac{1}{j\omega}, \tag{4}$$

where ω is the normalized frequency.

The measurement noises of the two microphones are uncorrelated. They are not affected by the differential operation. The accumulator acts as a low-pass filter to them. Therefore, a high-pass filter is inserted to improve the signal-to-noise ratio (SNR) of the DMA. Since the performance of the FBANC system is significantly influenced by the group delay in the secondary path, it is suggested to carry out this high-pass filter in an infinite impulse response (IIR) structure.

The beampattern of the DMA is given by

$$|B(\theta)| = \left| \frac{1 - e^{j\Omega\frac{\delta}{c}(1+\cos\theta)}}{2\Omega\frac{\delta}{c}} \right| \approx \frac{1}{2}(1 + \cos\theta), \tag{5}$$

where θ is the azimuthal angle; Ω denotes the angular frequency; c denotes the sound speed; and δ is the spacing between the two microphones in the DMA.

It is noted in (5) that the DMA consisting of two omni-directional microphones has a frequency-invariant cardioid beampattern. When the DMA is used to provide the error signal for the FBANC system, the null is configured to the direction of the interference. By doing so, the FBANC system improves its robustness against interferences. However, the output of the DMA presents the sound pressure gradient instead of the sound pressure. The DMA's location does not precisely indicate the control point where optimum noise reduction has been achieved.

C. Auxiliary filter based mapping method

To solve this problem, the AFMap method is developed in two stages, as shown in Fig. 3. S_1 and S_2 denote the transfer

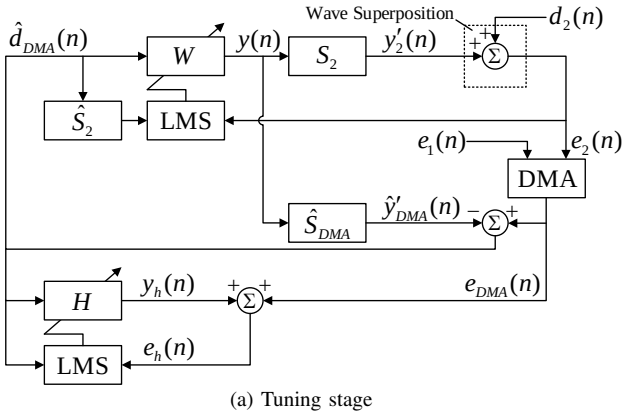

(a) Tuning stage

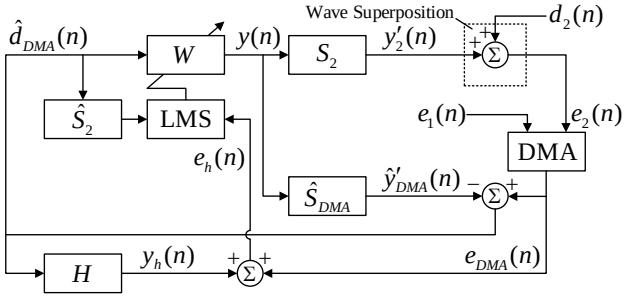

(b) Control stage

Fig. 3. Block diagram of the AFMap method.

functions from the secondary source to the two microphones in the DMA, respectively. $\hat{S}_2$ denotes an estimate of S_2. $\hat{S}_{DMA}$ denotes the estimated transfer function from the secondary source to the output of the DMA. H denotes the transfer function of the auxiliary filter. The AFMap method aims to map the differential error signal to the location of microphone 2. As the secondary path model related to microphone 1 is not required by the FBANC system, S_1 is not explicitly illustrated in Fig. 3.

In the tuning stage, the error signal $e_i(n)$ picked up by microphone i in the DMA is expressed as

$$e_i(n) = d_i(n) + \mathbf{y}(n) * \mathbf{s}_i(n), i = 1, 2, \tag{6}$$

where $d_i(n)$ and $\mathbf{s}_i(n)$ are the disturbance signal and the secondary path of microphone i, respectively.

The differential error signal, *i.e.* the output of the DMA, is denoted as $e_{DMA}(n)$. The input of the control filter is hence calculated as

$$x(n) \triangleq \hat{d}_{DMA}(n) = e_{DMA}(n) - \mathbf{y}(n) * \hat{\mathbf{s}}_{DMA}(n), \tag{7}$$

where $\hat{\mathbf{s}}_{DMA}(n)$ is the differential secondary path model.

The coefficients of the control filter and the auxiliary filter $\mathbf{h}(n)$ are updated by

$$\mathbf{w}(n+1) = \mathbf{w}(n) - \mu_w[\hat{\mathbf{s}}_2(n) * \mathbf{x}(n)]e_2(n) \tag{8}$$

and

$$\mathbf{h}(n+1) = \mathbf{h}(n) - \mu_h \mathbf{x}(n) e_h(n), \tag{9}$$

respectively. Furthermore, μ_h is the step size for the adaptation of the auxiliary filter, and $e_h(n)$ is written as

$$e_h(n) = e_{DMA}(n) + \mathbf{h}(n) * \mathbf{x}(n). \tag{10}$$

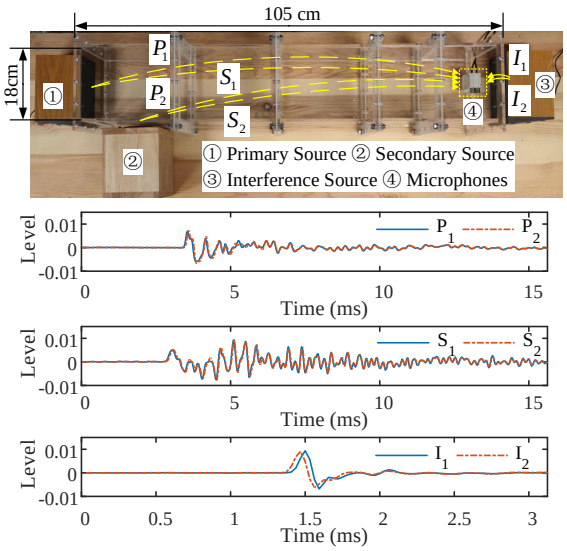

Fig. 4. Experiment setup and impulse responses of primary paths (P_1 and P_2), secondary paths (S_1 and S_2) and interference paths (I_1 and I_2).

In the control stage, the coefficients of the auxiliary filter have been well-trained. The coefficients of the control filter are updated by

$$\mathbf{w}(n+1) = \mathbf{w}(n) - \mu_w[\hat{\mathbf{s}}_{DMA}(n) * \mathbf{x}(n)]e_h(n). \tag{11}$$

The AFMap method is analyzed in the z domain as follows. In the tuning stage, the control filter converges to the optimal solution $W_o(z)$, which minimizes the power of the conventional error signal $e_2(n)$. Hence, the control point is localized at the location of microphone 2. Meanwhile, the auxiliary filter $H(z)$ converges to

$$H(z) = -[1 + \hat{S}_{DMA}(z)W_o(z)], \tag{12}$$

in order to contain the information regarding the optimal control filter. In the control stage, the z transform of $e_h(n)$ is derived as

$$\begin{aligned} E_h(z) &= \hat{D}_{DMA}(z)H(z) + E_{DMA}(z) \\ &\approx \hat{D}_{DMA}(z)\hat{S}_{DMA}(z)[W(z) - W_o(z)]. \end{aligned} \tag{13}$$

When the power of $e_h(n)$ is minimized, the control filter converges to the optimal control filter that achieves optimum noise reduction at the location of microphone 2 again.

III. Experiment Results

Experiments are carried out in an open end rectangular duct with three loudspeakers and two microphones. The first loudspeaker is mounted at one end of the duct as the primary source. The second loudspeaker is mounted at the side opening of the duct as the secondary source. Two microphones are placed near the open end of the duct. The third loudspeaker is placed outside the duct as the interference source. The experiment setup is shown in Fig. 4, where the impulse responses of the primary, secondary and interference paths are also plotted using a sampling rate of 32 kHz. The primary and secondary paths have the length of 500 taps, while the

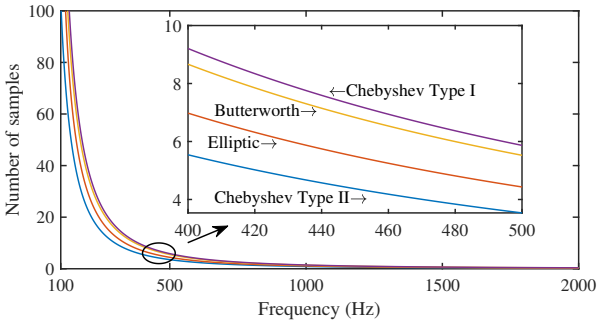

Fig. 5. Group delays of four types of high-pass IIR filters.

TABLE I
PARAMETERS.

Primary noise	400 Hz to 500 Hz
Primary noise level	80 dB
Weak interference level	69 dB
Strong interference level	89 dB
μ_w	3e-2
μ_h	4.5e-3
Length of the control filter	400 Taps
Length of the auxiliary filter	500 Taps
Length of secondary path models	500 Taps
Background noise level	35 dB

interference paths have the length of 100 taps. The relative time delay between the two microphones is estimated as 1.184 sampling intervals.

Four types of high-pass IIR filters, including the Butterworth, Elliptic, Chebyshev Type I and Type II, are designed under the same specifications. The passband frequency is 100 Hz and the ripple in the passband is 1 dB. The stopband frequency is 15 Hz and the attenuation in the stopband is 80 dB. The group delays of the four IIR filters are shown in Fig. 5, where the Chebyshev Type II filter exhibits the lowest group delay in the frequency band of the primary noise. Therefore, the Chebyshev Type II filter is adopted in the DMA processing.

The conventional and differential error FBANC systems are compared in Fig. 6 with different interference levels. The parameters used to achieve these results are listed in Table I. The FBANC systems are turned on after 30 seconds. A speech signal is used as the interference, lasting for 5 seconds. The noise reduction is always evaluated at the location of microphone 2, which is the error microphone of the conventional FBANC system.

In Fig. 6 (a), the conventional FBANC system achieves the highest noise reduction. When there is a weak interference in Fig. 6 (b), the overshoot of the conventional FBANC system is much higher than the differential error FBANC system. If the interference is strengthened, the conventional FBANC system may fail to work as a result of overflowing, as shown in Fig. 6 (c). The AFMap method demonstrates its effectiveness in the differential error FBANC system as it improves the noise reduction at the location of microphone 2. Figure 7 further shows the spectrograms at the location of microphone 2 with the presence of the strong interference. The differential error FBANC system inherits the drawback of the first-order DMA, where the low-frequency background noise is amplified. This

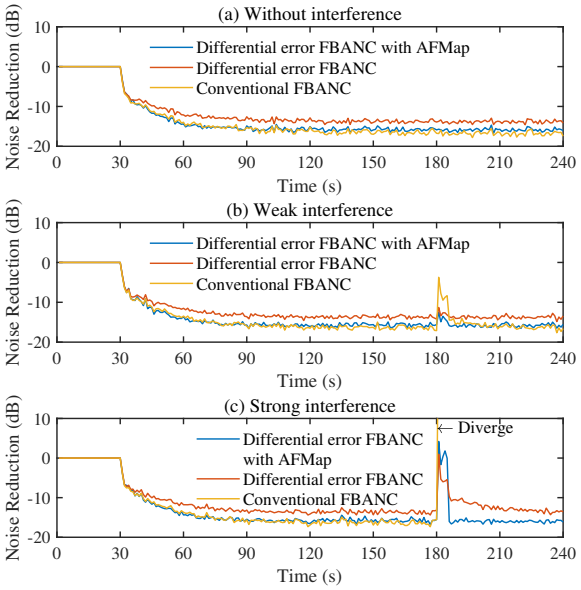

Fig. 6. Noise reduction of the conventional and differential error feedback ANC systems.

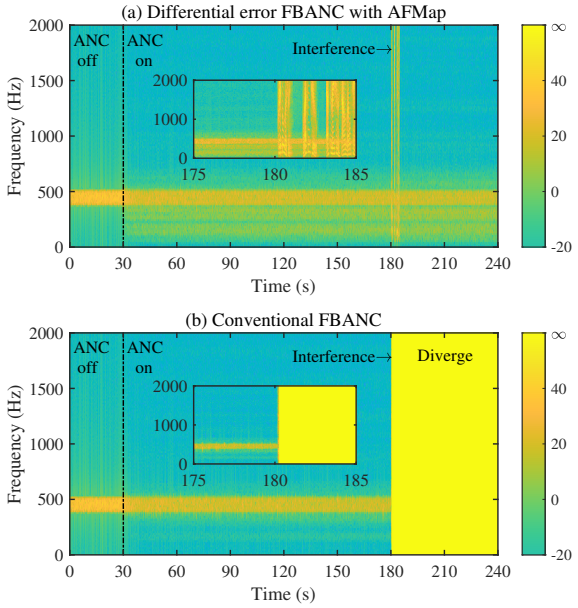

Fig. 7. Spectrograms at the location of the microphone 2 with the presence of the strong interference.

can be resolved by the fractional-order DMA in future [42].

IV. CONCLUSIONS

This letter proposes the differential error FBANC system using the DMA to mitigate interferences that interrupt the adaptation of the control filter in conventional FBANC systems. Because the location of the DMA cannot precisely indicate the control point where optimum noise reduction has been achieved, the AFMap method is developed to make the control point readily localized at the location of an omni-directional microphone in the DMA. Experiment results validate the effectiveness of the proposed differential error FBANC system with the AFMap method in an open end duct, against interferences of different levels.

REFERENCES

[1] S. M. Kuo and D. R. Morgan, *Active Noise Control Systems: Algorithms and DSP Implementations*, vol. 4, Wiley, New York, 1996.

[2] S. J. Elliott and P. A. Nelson, "Active noise control," *IEEE Signal Process. Mag.*, vol. 10, no. 4, pp. 12–35, 1993.

[3] S. M. Kuo and D. R. Morgan, "Active noise control: a tutorial review," *Proc. IEEE*, vol. 87, no. 6, pp. 943–973, 1999.

[4] C. H. Hansen, *Understanding Active Noise Cancellation*, vol. 1, Spon Press,London, 2001.

[5] Y. Kajikawa, W. S. Gan, and S. M. Kuo, "Recent advances on active noise control: open issues and innovative applications," *APSIPA Trans. Signal Inf. Process*, vol. 1, pp. 1-21, 2012.

[6] S. J. Elliott, *Signal Processing for Active Control*, Academic Press: London, 2000.

[7] S. J. Elliott and T. J. Sutton, "Performance of feedforward and feedback systems for active control," *IEEE. Trans. Speech Audio Process.*, vol. 4, no. 3, pp. 214–223, 1996.

[8] K. Iwai, S. Kinoshita, and Y. Kajikawa,, "Multichannel feedforward active noise control system combined with noise source separation by microphone arrays," in *J. Sound Vib.*, vol. 453, pp 151-173, 2019.

[9] T. Murao, C. Shi, W. S. Gan, and M. Nishimura, "Mixed-error approach for multi-channel active noise control of open windows," *Appl. Acoust.*, vol. 127, pp. 305-315, 2017.

[10] B. Lam, C. Shi, D. Shi, and W. S. Gan, "Active control of sound through full-sized open windows," *Build. Environ.*, vol. 141, pp. 16-27, 2018.

[11] T. Wang and W. S. Gan, "Stochastic analysis of fxlms-based internal model control feedback active noise control systems," *Signal Process*, vol. 101, pp. 121–133, 2014.

[12] S. M. Kuo, S. Mitra, and W. S. Gan, "Active noise control system for headphone applications," *IEEE Trans. Control Sys. Technol.*, vol. 14, no. 2, pp. 331–335, 2006.

[13] C. Shi, Z. Jia, R. Xie, and H. Li, "Effect of cross-channel control filters in multi-channel feedback active noise control," in *Proc. 12th Asia Pacific Signal and Information Processing Association Annual Summit and Conference*, 2020.

[14] W. S. Gan, S. Mitra, and S. M. Kuo, "Adaptive feedback active noise control headset: implementation, evaluation and its extensions," *IEEE Transactions on Consumer Electronics*, vol. 51, no. 3, pp. 975–982, 2005.

[15] X. Kong, P. Liu, and S. M. Kuo, "Multiple channel hybrid active noise control systems," *IEEE Trans. Control Sys. Technol.*, vol. 6, no. 6, pp. 719–729, 1998.

[16] K. Beemanpally, K. R. Pottim, and S. M. Kuo, "Multi-channel hybrid active noise control system for infant incubators," in *IEEE Int. Conf. on Electro/Information Technology*, 2010, pp. 1–8.

[17] O. J. Tobias, J. C. M. Bermudez, and N. J. Bershad, "Mean weight behavior of the filtered-x lms algorithm," *IEEE Trans. Signal Process.*, vol. 48, no. 4, pp. 1061–1075, 2000.

[18] O. J. Tobias and R. Seara, "Leaky-fxlms algorithm: stochastic analysis for gaussian data and secondary path modeling error," *IEEE Trans. Speech Audio Process.*, vol. 13, no. 6, pp. 1217–1230, 2005.

[19] D. Shi, W. S. Gan, B. Lam, and K. Ooi, "Fast adaptive active noise control based on modified model-agnostic meta-learning algorithm," *IEEE Signal Process. Lett.*, vol. 28, pp. 593–597, 2021.

[20] D. Shi, W. S. Gan, B. Lam, and C. Shi, "Two-gradient direction fxlms: An adaptive active noise control algorithm with output constraint," *Mech. Syst. Signal Process.*, vol. 116, pp. 651–667, 2019.

[21] S. J. Elliott, I. M. Stothers, and P. A. Nelson, "A multiple error LMS algorithm and its application to the active control of sound and vibration," *IEEE Trans. Acoust. Speech Sig. Process.*, vol. 35, no. 10, pp. 1423–1434, 1987.

[22] S. K. Tang and J. S. F. Cheng, "On the application of active noise control in an open end rectangular duct with and without flow," *Appl. Acoust.*, vol. 53, no. 1-3, pp. 193-210, 1998.

[23] J. Benesty and J. Chen, *Study and Design of Differential Microphone Arrays*. Berlin, Germany: Springer-Verlag, vol.6, 2012.

[24] X. Leng, J. Chen, and J. Benesty, "A new method to design steerable first-order differential beamformers," *IEEE Signal Process. Lett.*, vol. 28, pp. 563–567, 2021.

[25] L. Zhao, J. Benesty, and J. Chen, "Optimal design of directivity patterns for endfire linear microphone arrays," in *Proc.40th IEEE Int. Conf. Acoust., Speech, Signal Process.*, 2015, pp. 295–299.

[26] E. De Sena, H. Hacihabiboglu, and Z. Cvetkovic, "On the design and implementation of higher order differential microphones," *IEEE Trans. Audio, Speech, Lang. Process.*, vol. 20, no. 1, pp. 162–174, 2012.

[27] G. Huang, J. Benesty, I. Cohen, and J. Chen, "A simple theory and new method of differential beamforming with uniform linear microphone arrays," *IEEE/ACM Trans. Audio, Speech, Lang. Process.*, vol. 28, pp. 1079–1093, 2020.

[28] G. Huang, J. Benesty, and J. Chen, "On the design of frequency-invariant beampatterns with uniform circular microphone arrays," *IEEE/ACM Trans. Audio, Speech, Lang. Process.*, vol. 25, no. 5, pp. 1140–1153, 2017.

[29] J. Jin, G. Huang, X. Wang, J. Chen, J. Benesty, and I. Cohen, "Steering study of linear differential microphone arrays," *IEEE/ACM Trans. Audio, Speech, Lang. Process.*, vol. 29, pp. 158-170, 2021.

[30] C. Pan, J. Chen, and J. Benesty, "Theoretical analysis of differential microphone array beamforming and an improved solution," *IEEE/ACM Trans. Audio, Speech, Lang. Process.*, vol. 23, no. 11, pp. 2093–2105, 2015.

[31] X. Wu, H. Chen, J. Zhou, and T. Guo, "Study of the mainlobe misorientation of the first-order steerable differential array in the presence of microphone gain and phase errors," *IEEE Signal Process. Lett.*, vol. 21, no. 6, pp. 667–671, 2014.

[32] Y. Buchris, I. Cohen, and J. Benesty, "Frequency-domain design of asymmetric circular differential microphone arrays," *IEEE/ACM Trans. Audio, Speech, Lang. Process.*, vol. 26, no. 4, pp. 760–773, 2018.

[33] D. Moreau, B. Cazzolato, A. Zander, and C. Petersen, "A review of virtual sensing algorithms for active noise control," *Algorithms*, vol. 1, no. 2, pp. 69–99, 2008.

[34] N. Miyazaki and Y. Kajikawa, "Adaptive feedback ANC system using virtual microphones," in *Proc. 38th IEEE Int. Conf. Acoust., Speech, Signal Process.*, 2013, pp. 383–387.

[35] N. Miyazaki and Y. Kajikawa, "Head-mounted active noise control system with virtual sensing technique," *J. Sound Vib.*, vol. 339, pp. 65–83, 2015.

[36] C. Shi, R. Xie, N. Jiang, H. Li, and Y. Kajikawa, "Selective virtual sensing technique for multi-channel feedforward active noise control systems," in *Proc. 44th IEEE Int. Conf. Acoust., Speech, Signal Process.*. 2019, pp. 8489–8493, IEEE.

[37] C. Shi, Z. Jia, R. Xie, and H. Li, "An active noise control casing using the multi-channel feedforward control system and the relative path based virtual sensing method," *Mech. Syst. Signal Process.*, vol. 144, pp. 106878, 2020.

[38] J. Garcia-Bonito, S. J. Elliott, and C. C. Boucher, "Generation of zones of quiet using a virtual microphone arrangement," *J. Acoust. Soc. Amer*, vol. 101, no. 6, pp. 3498–3516, 1997.

[39] S. J. Elliott and J. Cheer, "Modeling local active sound control with remote sensors in spatially random pressure fields," *J. Acoust. Soc. Amer*, vol. 137, no. 4, pp. 1936–1946, 2015.

[40] S. J. Elliott, W. Jung, and J. Cheer, "Causality and robustness in the remote sensing of acoustic pressure, with application to local active sound control," in *Proc. 44th IEEE Int. Conf. Acoust., Speech, Signal Process.*, 2019, pp. 8484–8488.

[41] T. I. Laakso, V. Valimaki, M. Karjalainen, and U. K. Laine, "Splitting the unit delay [FIR/all pass filters design]," *IEEE Signal Process. Mag.*, vol. 13, no. 1, pp. 30–60, 1996.

[42] G. Huang, J. Chen, and J. Benesty, "Design of planar differential microphone arrays with fractional orders," *IEEE/ACM Trans. Audio, Speech, Lang. Process.*, vol. 28, pp. 116-130, 2020.